Biliverdin-copper complex at physiological pH

Dimitrijević, Milena S.; Bogdanović Pristov, Jelena; Žižić, Milan; Stanković, Dalibor M.; Bajuk-Bogdanović, Danica; Stanić, Marina; Spasić, Snežana; Hagen, Wilfred; Spasojević, Ivan

DOI
10.1039/c8dt04724c

Publication date
2019

Document Version
Accepted author manuscript

Published in
Dalton Transactions

Citation (APA)
Dimitrijević, M. S., Bogdanović Pristov, J., Žižić, M., Stanković, D. M., Bajuk-Bogdanović, D., Stanić, M., Spasić, S., Hagen, W., & Spasojević, I. (2019). Biliverdin-copper complex at physiological pH. *Dalton Transactions*, *48*(18), 6061-6070. https://doi.org/10.1039/c8dt04724c

Biliverdin-copper complex at physiological pH

Milena Dimitrijević,[1] Jelena Bogdanović Pristov,[1] Milan Žižić,[1] Dalibor M. Stanković,[2,3] Danica Bajuk-Bogdanović,[4] Marina Stanić,[1] Snežana Spasić,[3] Wilfred Hagen,[5] Ivan Spasojević[1*]

[1]*Institute for Multidisciplinary Research, University of Belgrade, Kneza Višeslava 1, 11030 Belgrade, Serbia*

[2] *The Vinča Institute of Nuclear Sciences, University of Belgrade, POB 522, 11001 Belgrade, Serbia*

[3]*Innovation Center of the Faculty of Chemistry, University of Belgrade, Studentski trg 12-16, 11158 Belgrade, Serbia*

[4]*Faculty of Physical Chemistry, University of Belgrade, Studentski trg 12-16, 11158 Belgrade, Serbia*

[5]*Department of Biotechnology, Delft University of Technology, Van der Maasweg 9, 2629HZ Delft, The Netherlands*

*Corresponding author: Ivan Spasojević

E-mail: : redoxsci@gmail.com

Abstract

Biliverdin (BV), a product of heme catabolism, is known to interact with transition metals, but the details of such interactions under physiological conditions are scarce. Herein, we examined coordinate/redox interactions of BV with Cu^{2+} in phosphate buffer at pH 7.4, using spectrophotometry, ESI-MS, Raman spectroscopy, ^{1}H NMR, EPR, fluorimetry, and electrochemical methods. BV formed a stable coordination complex with copper in 1:1 stoichiometry. The structure of BV was more planar and energetically stable in the complex. The complex showed strong paramagnetic effects that were attributed to an unpaired delocalized e^{-}. The delocalized unpaired electron most likely comes from BV, so the complex is formally composed of BV radical cation and Cu^{1+}. The complex underwent oxidation only in the presence of both O_2 and an excess of Cu^{2+}, or by a strong oxidizing agent, and it was resistant to reducing agents. The biological effects of the stable BV metallocomplex containing a delocalized electron should be further examined, and may provide an answer to the long-standing question of high energy investment in the catabolism of BV, which represents a relatively harmless molecule *per se*.

Introduction

Heme, iron protoporphyrin IX complex, is released from hemoglobin in senescent and impaired erythrocytes.[3] It is further subjected to enzymatic degradation to biliverdin (BV) that is rapidly converted to bilirubin by BV reductase. It is still not clear why physiologically harmless BV, which may be easily excreted without conjugation,[4] requires energetically expensive two-electron reduction to potentially toxic bilirubin.[5] A potential explanation may reside in the coordinate and/or redox interactions of BV with copper and other physiologically-relevant metals, which have been extensively studied by the Balch's group and others [2, Nguyen, Balch 1993, Balch 1994, Balch 1992, Spasojevic 2001]. However, the interactions of BV with copper ions have not been examined using physiological settings. Previous studies have preformed the synthesis/analysis of BV-copper complexes in organic solvents,[2,6] in aqueous medium at a very high pH,[6-7] or using Tris buffer,[8] which shows high affinity for Cu^{2+} and may interfere with the interactions with BV.[9]

In the present study we applied spectroscopic, (para)magnetic resonance, and electrochemical methods to elucidate the structure and redox properties of complex of BV with copper ions under physiological conditions using phosphate buffer at pH 7.4. Our results imply the formation of a BV radical – copper complex containing a delocalized unpaired electron.

Experimental section

Chemicals

All chemicals were of analytical grade: BV, buffer components, dimethyl sulfoxide (DMSO), DMSO-d6 (deuterated DMSO, 99.9 % D atom), D_2O (99.9 % D atom), and urea were purchased from Sigma-Aldrich (St. Louis, MO, USA); $CuCl_2$ was from Merck (Kenilworth, NJ, USA); solvents for MS (acetonitrile, formic acid; LC–MS grade) were obtained from Fisher Scientific (Loughborough, UK). All experiments were performed using bidistilled deionized water (18 MΩ) that was obtained by reagent grade water system (Millipore, Billerica, USA). Stock solutions of BV - 20 mM in DMSO for experiments with high final concentrations (NMR, Raman, CV) or 1 mM in 5 mM NaOH for all other experiments were prepared daily and kept on ice in the dark. Phosphate buffer - 50mM K_2HPO_4 with pH adjusted to 7.4 with KOH, was prepared daily.

UV-VIS spectroscopy

UV-Vis absorption spectra were obtained using a 2501 PC Shimadzu spectrophotometer (Kyoto, Japan). Sample volume was 1 mL. Scan time was 50 s. Samples were freshly prepared and immediately scanned at wavelengths from 800 to 200 nm at room T. Changes of spectra were monitored for 60 min. Each system was prepared in light-protected glass and stirred. Aliquots were measured and discarded for each time-point, since we noted that irradiation during the collection of UV-Vis spectra may result in BV degradation.

ESI-MS spectrometry

MS analysis was performed using a TSQ Quantum Access Max mass spectrometer equipped with a HESI source, which was used with ion source settings as follows: spray voltage, 3500 V; sheath gas, N_2; pressure, 30 AU; ion sweep gas pressure, 3 AU; auxiliary gas (N_2) pressure, 10 AU; vaporizer temperature, 450°C; capillary temperature, 380°C; skimmer offset, 0 V. Multiple mass spectrometric data were acquired in positive mode, including full scanning in *m/z* range from 100 to 1000 (FS) for qualitative analysis and product ion scanning (PIS) mode for the quantitative analysis. Collision–induced fragmentation experiments were performed using Ar as the collision gas, with collision energy set at 5 eV. SRM experiments for quantitative analysis was performed using two MS2 fragments for each compound, which were previously defined as dominant in PIS experiments. Standard calibration curves were generated using equal–weighted linear regression and external standard method for quantification of each compound. Samples were introduced into the mass spectrometer with a syringe pump and continuous flow injection for a period of 5 min at a flow rate of 5.0 μL/min. Analyst version 1.4 of Xcalibur software (Thermo Fisher Scientific, Bremen, Germany) was used for data acquisition and processing.

Raman spectroscopy

The Raman spectra of sample solutions were recorded on a Thermo DXR Raman microscope (Thermo Fisher Scientific, Waltham, MA, USA). Aliquots of 5 μL os sample were placed on the Raman grade calcium fluoride holder following the adjustment and stabilization of pH of the solution and 5 min incubation period, and Raman spectra were recorded. The 532 nm laser excitation line was used, with the following settings: exposure time, 10 s; number of exposures, 10; grating, 900 lines/mm; pinhole, 50 μm; laser power at the sample, 2 MW.

Fluorescence Spectroscopy

Fluorescence spectra were acquired using a Fluorolog FL3-221 with a 450 mW Xe lamp (Jobin Yvon Horiba, Paris, France), and FluorEssence 3.5 software (Horiba Scientific, Kyoto, Japan),

and the following settings: excitation range, 320–400 nm; emission range, 400–600 nm; increment, 2 nm; slit (band pass), 3 nm for establishing excitation and emission spectra, and 1 nm for acquiring emission spectra at 293 K and 328 K, and emission spectra in the presence of urea (5 M). Emission detector signal was scaled by reference quantum counter signal (S1/R1). Lifetime was calculated from fluorescence decay profile which was established using excitation nano-led diode (380 nm). The emission was detected at 470 nm and 480 nm for BV and BV/Cu system, respectively. The decay was fitted using 3 exponentials. Relative quantum yield was determined from emission and excitation spectra using FluorEssence 3.5 software.

^{1}H NMR Spectroscopy

^{1}H NMR spectra of BV (300 μM) in the absence or in the presence of $CuCl_2$ (300 μM) were recorded on a Bruker Avance III 500 spectrometer with TopSpin v3.2 interface, using 5 mm BBO probe-head, at 298 K. All samples (and solutions) were prepared in D_2O and placed in 5-mm quartz tubes. Residual HDO signal at 4.7 ppm was used as chemical shift reference. Spectra were analyzed in MestReNova 12.0.1 (Mestrelab Research, Santiago de Compostela, Spain).

EPR Spectroscopy

Perpendicular-mode EPR spectra at 30 K were recorded on a Bruker Elexsys-II EPR spectrometer operating at X-band (9.616 GHz), using the following conditions: power, 32 dB; modulation amplitude, 0.8 mT; modulation frequency, 100 kHz. Parallel-mode signals were obtained at 25.5 K, using a Bruker EMXplus spectrometer operating at X-band (9.272 GHz) with the dual-mode cavity, and the following settings: power, 16 or 32 dB; modulation amplitude, 1 mT; modulation frequency, 20 kHz. Samples were placed in quartz EPR tubes and quickly frozen in cold isopentane following 5 min incubation period under anaerobic conditions. All spectra were non-saturated and baseline corrected. Measurements at room T were conducted on a Varian E104 operating at X-band (9.51 GHz), using the following settings: microwave power, 20 mW; modulation amplitude, 0.2 mT; modulation frequency, 100 kHz. Spectra were obtained under aerobic conditions. The simulation of the room T EPR spectrum was performed in WINEPR SimFonia software (Bruker Analytische Messtechnik GmbH, Darmstadt, Germany), using previously described parameters [Peeks].

Oximetry

Concentration of O_2 in samples was measured/monitored using a Clark type oxygen electrode (Hansatech Instruments Ltd., King's Lynn, UK) operating with Lab Pro interface and Logger Pro

3 software (Vernier, Beaverton, OR, USA). All systems were recorded for 2-5 min before the addition of Cu to establish the stability of baseline and zero rate of O_2 change at room T.

Cyclic voltammetry and differential pulse voltammetry

The voltammetric measurements were performed using a potentiostat/galvanostat CHI 760b (CH Instruments, Inc, Austin, TX, USA). The electrochemical cell (total volume of 3 mL) was equipped with a boron-doped diamond electrode (surface area 7.07 mm^2; Windsor Scientific LTD, UK; declared performances: resistivity, 0.075 Ω cm; boron doping level, 1000 ppm), as the working electrode, an Ag/AgCl (3M KCl) and platinum wire as reference and counter electrode, respectively. All potentials reported in this paper are referred versus this electrode. Scan rate was 0.1 V/s. Differential pulse voltammetry was performed on the same instrument using the following settings: initial *E*, -1 V; final *E*, 1 V; increment, 0.004 V; amplitude, 0.05 V; pulse width, 0.05 s; sample width, 0.01 s; quiet time, 2 s. Measurements were initiated immediately after sample preparation and performed at room T.

Results and discussion

UV-Vis spectrophotometry was applied to investigate formation/degradation of complex of BV with copper ions at pH 7.4 (Fig. 1). BV showed bands with λ_{max} at 315 nm (non-restricted open-chain bilatriens), 375 nm (Soret-like band), and 670 nm (transitions in C═C and C═N systems).[10] Different [BV]/[Cu^{2+}] concentration ratios were applied to evaluate the stoichiometry (Fig. 1a). At [BV]/[Cu^{2+}] = 2, an immediate decrease in the intensity of the λ_{670} absorption band was observed. At [BV]/[Cu^{2+}] = 1, the λ_{670} band was absent, whereas the λ_{375} peak was shifted to 400 nm. The spectrum for [BV]/[Cu^{2+}] = 2 corresponded to the sum of the experimental spectra for [BV]/[Cu^{2+}] = 1 and BV. The signal in the presence of an excess of Cu^{2+} ([BV]/[Cu^{2+}] = 0.5) was similar to the [BV]/[Cu^{2+}] = 1 system. Altogether, this implies that BV interacted with Cu^{2+} in 1:1 stoichiometry, which was further confirmed by titration (Fig. 1e). The reaction was over within 5 min and all signals were stable under anaerobic conditions for at least one hour. The [BV]/[Cu^{2+}] = 2 system was also stable in the presence of O_2 (Fig. 1b), which implies that the complex is not susceptible to oxidation by O_2 *per se*. On the other hand, signals for [BV]/[Cu^{2+}] = 1 and [BV]/[Cu^{2+}] = 0.5 systems showed a decay with time under aerobic settings (Fig. 1c, d). The decrease was more pronounced for the latter. It appears that the complex undergoes oxidation/degradation only in the presence of both O_2 and 'free' Cu^{2+}. The latter is present in

traces for the [BV]/[Cu^{2+}] = 1 system, and in excess for [BV]/[Cu^{2+}] = 0.5. In the [BV]/[Cu^{2+}] = 2 system, BV sequestered (almost) all available copper thus preventing the oxidation. The sensitivity of complexes of Cu^{2+} and porphyrin model molecules to O_2 has been observed previously in organic solvents.[2,6,11] However, the involvement of 'free' Cu^{2+} has not been taken into consideration. It is important to point out that the complex was not affected by bathocuproine, a copper chelating agent (Fig. S1), implying that copper cannot be easily removed from the complex. Further, we observed that BV degradation at [BV]/[Cu^{2+}] = 1 molar ratio was promoted at higher BV and Cu^{2+} concentrations (Fig. S2). This is most likely related to a higher amount of 'free' copper ions and/or to a different Cu^{2+} speciation in phosphate buffer for different [Cu^{2+}] (Fig. S3). The degradation of the complex at high concentrations was prevented by an excess of BV (in the [BV]/[Cu^{2+}] = 2 system). Therefore, we applied a [BV]/[Cu^{2+}] = 2 molar ratio for methods/measurements that required high concentrations and longer recording periods at room T. It is worth mentioning that the interactions of porphyrins with metals are frequently studied in DMSO, which is a more convenient solvent for some analyses. BV showed similar UV-Vis spectra in DMSO and phosphate buffer (Fig. S4). On the other hand, spectral features of the [BV]/[Cu^{2+}] = 1 system differed significantly. The 660 nm band was not annihilated in the presence of equimolar Cu^{2+} concentration, whereas the 380 nm band showed a decrease and developed a "shoulder" at approximately 440 nm. This showed that the interactions of BV with Cu^{2+} in DMSO and in phosphate buffer differ, and pointed out the importance of analysing BV/Cu^{2+} system in the aqueous medium.

ESI-MS analysis confirmed that BV built a complex with copper ions in 1:1 stoichiometry (Fig. 2a). The mass spectrum of BV showed a molecular ion peak at 583.07 $[M + H^+]^+$. In the presence of Cu^{2+} in 1:1 molar ratio, a peak at 643.36 emerged, whereas the peak of free BV was absent. This *m/z* value corresponds to the sum of masses of BV and copper $[(M + Cu^{2+} - H^+]^+$. ESI-MS of the [BV]/[Cu^{2+}] = 0.5 system showed a significantly higher number of detectable fragments compared to other systems (Fig. S5). It is noteworthy that the observed *m/z* of ~264 and ~320 could be assigned to a propentdyopent and its complex with copper, which have been reported to form from BV analogs (bilindiones) in the presence of copper and oxygen.[2] Next, we applied Raman spectroscopy (Fig. 2b). The Raman spectrum of BV was in good agreement with previous reports (Table S1). Comparing spectra of BV and BV-Cu complex, the following differences were observed: (i) a new band at 540 cm^{-1} emerged for the complex; (ii) the band at

844 cm^{-1} was shifted to 821 cm^{-1}; (iii) the peak at 1303 cm^{-1} was (almost) absent; (iv) the band at 1333 cm^{-1} was stronger; (v) the line at 1480 cm^{-1} was stronger; (vi) it appears that two peaks/shoulders of 1616 cm^{-1} band emerged/were stronger at ~1580 cm^{-1} and ~1630 cm^{-1}. The 540 cm^{-1} band may be attributed to Cu-N bond vibration.[12] The band at 844 cm^{-1} was attributed to ring (C-C bond) stretching.[13] The shift to lower energies implicates increased stability of BV in the complex. The band at 1303 cm^{-1} may be attributed to wagging vibration of C-H bond,[13] which are very sensitive to environmental factors.[14] The 1333 cm^{-1} band has been previously recognized as a structure-sensitive band for Cu-bilirubin complex, and has been attributed to $CH(CH_3)$ in-plane vibration.[13,15] Therefore, changes in the intensities of these two bands imply a more planar structure of BV in the complex. Stronger bands at 1480 cm^{-1} (stretching of aliphatic C-C bonds), ~1580 cm^{-1} (stretching of C=C bonds in the ring), and ~1630 cm^{-1} (stretching of C=C and C=O bonds in the ring), imply higher delocalization of π-electrons and consequently a higher stability of the BV structure. Pertinent to this, it has been proposed that complexes of BV model compounds with Cu^{2+} may show unusual electronic structures that exhibit a significant ligand radical character.[24]

Figure 3a shows ^1H NMR spectrum of BV in phosphate buffer (prepared with D_2O). Poor resolution of signals, which may originate from aggregation [Feliz], did not allow reliable assignment. However, this was of little relevance here, since the addition of copper ions led to a very strong effect - the complete loss of almost all lines. The loss of signals represents a result of strong paramagnetic effects that may come from an unpaired e^- that is delocalized in pπ orbitals of the ring influencing all protons in the complex. It is worth mentioning that ^1H NMR lines of BV in deuterated DMSO were comparatively well resolved (Fig. S6), which points to an alteration of the protonation state and/or location, and in particular to different aggregation pattern. In addition, the lines were not lost in the presence of even higher Cu^{2+} concentration (Fig. S6), underpinning the significant difference in BV/Cu^{2+} interactions in the two media. Low-T EPR was applied to further examine paramagnetic properties of the BV-Cu complex. The EPR spectrum of Cu^{2+} (S = 1/2; I = 3/2) in phosphate buffer shows that Cu^{2+} is weakly coordinated in an axial symmetry with one $g_\perp$ line and four lines coming from hyperfine coupling along $g_\parallel$ (Fig. 3b). The addition of BV in equimolar concentration led to the loss of Cu^{2+} signal. In the [BV]/[Cu^{2+}] = 0.5 system the double integral of the signal of Cu^{2+} in phosphate buffer was decreased by half, implying that that an excess of copper is not bound to BV. The remaining

signal in the [BV]/[Cu^{2+}] = 1 system was broad, and did not show hyperfine structure. The *g*-value of the isotropic signal of BV-Cu complex was significantly lower than the average *g*-value of Cu^{2+} in the phosphate buffer indicating delocalizaton of the spin away from the metal nucleus. Similar EPR signals have been reported previously for porphyrin radical cation [Peeks], and for an oxidized copper-porphyrin model molecule complex.[21] The signals have been attributed to a highly delocalized electron [[21] Peeks]. In addition, the [BV]/[Cu^{2+}] = 1 system showed a 9-line EPR spectrum at room T (Fig. 3c), as previously reported for porphyrin radical cation by Peeks and co-workers [Peeks]. The simulation of this signal was performed assuming four equivalent ^{14}N nuclei with an isotropic hyperfine coupling constant of 0.14 mT [Peeks]. This speaks in favour of a delocalization of unpaired electron over the complex center. Finally, parallel-mode EPR showed no signal (Fig. 3d). Furthermore, the spectra were ran over a wide field range and no half field lines were observed, either in parallel or in perpendicular mode. These results are consistent with $S = 0$ for the copper center.

Next, we compared the fluorescence of BV and BV-Cu complex (Fig. 3e-h). The [BV]/[Cu^{2+}] = 1 system showed about two-fold stronger fluorescence compared to BV at equimolar concentration (Fig. 3e). Relative quantum yields for BV and BV-Cu complex were 0.86 and 0.95, respectively. However, the excitation and emission maxima, as well as the lifetimes were next-to-identical (Fig. 3f), which implies that the fluorecence comes form the same fluorophore(s). To check whether the difference in fluorescence intensity is related to aggregation-caused quenching, we applied temperature increase and 5 M urea to induce deaggregation [Feliz, Rahman]. The increased fluorescence of BV under deaggregating conditions confirmed that BV forms aggregates in phosphate buffer (Fig. 3g, h), as proposed regarding the resolution of ^{1}H NMR spectrum of BV (Fig. 3a). On the other hand, no changes were observed for BV-Cu complex, which implies that it did not form aggregates. This may be explained by a more planar structure and electrostatic repulsion by redistributed charge of the complex. It is important to note that the results obtained by fluorimetry further confirm that copper in the BV-Cu complex is not present in a paramagnetic form (Cu^{2+} with $S = 1/2$ or Cu^{3+} with $S = 1$). The paramagnetic nature of Cu^{2+} (or high-spin Cu^{3+} in analogy with Ni^{2+}) may lead to quenching by enhancing the processes that compete with fluorescence, such as intersystem crossing and spin–orbit coupling.[17,18]

Further, redox properties of the complex were examined. BV showed a well-defined anodic peak at E_{pa1} = 117 mV (Fig. 4a). CV of Cu^{2+} in phosphate buffer showed reversible redox behavior at a peak potential at ~ -0.4 V, with very weak currents. Therefore, the redox activity of BV-Cu systems in cyclic voltammograms was complex-centered. The [BV]/[Cu^{2+}] = 2 system showed two additional oxidation peaks at much lower potentials than BV: E_{pa2} = -91 mV and E_{pa3} = -341 mV. The former potential corresponds to the oxidation of Cu^{1+}, as we have shown previously [Bozic]. No reduction peaks could be observed. Differential pulse voltammetry delivered similar results – the [BV]/[Cu^{2+}] = 2 system showed two additional peaks, most likely coming from two $1e^-$ oxidations (Fig. 4b). It is noteworthy that a similar oxidation pattern has been observed previously for a complex of BV model compound with copper.[25] A direct linear relationship between *I* and the square root of scan rate implies that the currents mainly depend on two parameters: the rate at which redox species diffuse to the electrode surface (*D*), and the rate constant of electron transfer (Fig. S7). Other interactions, for example adsorption, were negligible.[27] BV showed significantly higher *D* compared to *D* values that were calculated for the two other peak currents. A faster diffusion of BV to the electrode surface in comparison to the BV-Cu complex was expected, since BV has more negative charge (two carboxyl groups are deprotonated at pH 7.4[28]), than the complex formed with positive copper ion. Oximetry was applied to examine the possibility that in the reaction between BV and Cu^{2+} an electron is lost, as proposed previously for complexes of copper ions with BV model molecules.[2,23] However, the syntheses have been performed in deaerated organic solvents, and in some cases it involved photo-oxidation and transmetalation of the model molecule. In the process, BV-type molecules act as non-innocent ligands and the complex may lose an electron to solvent molecules or acetate ($Cu(CH_3COO)_2$ is commonly used for the synthesis). In the settings applied here, molecular oxygen is the final e^- acceptor. It may be directly involved in redox reaction between BV and Cu^{2+}, or it may be reduced by Cu^{1+}, which is unstable under physiological settings. There was a slight consumption of O_2 in [BV]/[Cu^{2+}] = 1 system during the process (Fig. 4c), which may be explained by traces of 'free' copper as discussed for Fig. 1 and Fig. S2. However, in the presence of an excess of copper ([BV]/[Cu^{2+}] = 0.5), the consumption of O_2 was significant. This implies that 'free' Cu^{2+} reacts with the complex and 'shuttles' an e^- to O_2. The addition of catalase to [BV]/[Cu^{2+}] = 0.5 system following 15 min incubation, resulted in O_2 release (not shown), implying that hydrogen peroxide is accumulated. As an illustration of the redox mechanism, we

added Cu^{1+} to the buffer. Cu^{1+} rapidly reduced O_2 at pH 7.4 to produce superoxide radical anion, which resulted in a drop of O_2 concentration. Next, the effects of reducing (Cu^{1+} and ascorbate) and oxidizing ($KMnO_4$) agents on BV-Cu complex were examined. The complex was not affected by Cu^{1+} (Fig. 4d). BV was exposed to a 1/1 mixture of Cu^{1+} and Cu^{2+} under anaerobic conditions. The spectrum of 20 μM BV with 10 μM Cu^{2+} and 10 μM Cu^{1+} corresponded to the spectrum of an analogous [BV]/[Cu^{2+}] = 2 system. Initially present Cu^{1+} did not affect the spectrum, and the system was stable. When exposed to air, Cu^{1+} was oxidized by O_2 to produce Cu^{2+} that reacted with free BV producing an additional amount of complex. The complex was not affected by ascorbate as well (Fig. 4e). On the other hand, the complex was degraded by $KMnO_4$, whereas this strong oxidizing species did not affect free BV (Fig. 4f).

The results presented here imply that BV and Cu^{2+} react under physiologcial settings to produce a 1:1 complex that is composed of Cu^{1+} and BV radical cation ($BV^{\cdot+}$). It should be stressed that the proposed distribution of electrons is formal, and that the unpaired e^- may be delocalized over the entire complex including the copper center. An electron is transferred form BV to copper, so a delocalized unpaired electron remains on the ring, whereas Cu^{1+} is bound to N in pyrroles. The presence of an unpaired delocalized e^- and the development of $BV^{\cdot+}$ are implicated by: (i) the results of Raman spectroscopy implicating a higher stability of BV in the complex that is provided by an additional delocalization of π-electronic cloud; (ii) NMR data showing strong paramagnetism of the complex; and (iii) perpendicular-mode EPR spectra. The proposed redox state of copper in the complex – Cu^{1+} is implicated by: (i) parallel-mode EPR and fluorescence results that were consistent with S = 0; (ii) The oxidation peak in CV of BV-Cu complex that corresponds to Cu^{1+} oxidation; and (iii) the susceptibility of the complex to oxidizing and not to reducing agents, since it appears more plausible that metal center and not delocalized e^- represents the main site of redox interactions of the complex. It is important to note that in addition to the reduction of Cu^{2+} to Cu^{1+} with concomitant formation of $BV^{\cdot+}$, a complex with delocalized e^- and copper with S = 0 may develop via another redox process: the oxidation of Cu^{2+} to Cu^{3+} that may show S = 0 (in addition to high-spin S = 1), and the formation of BV radical anion. However, previous studies have shown that BV as well as trianionic corroles may reduce Cu^{3+} [Wasbotten, Pierloot]. Pertinent to this, it appears that a complex between reduced BV and Cu^{3+} would not be stable.

Conclusions

At physiological pH, BV builds a complex with copper ions in 1:1 stoichiometry. The formation of complex involves the rearrangement of electronic structure which provides increased energetic stability and strong paramagnetic effects. We believe that a complex with a highly delocalized unpaired e^- and the formal $BV^{\cdot+}$-Cu^{1+} character best suites the outlined properties, but other structures of the complex cannot be completely ruled out. The presented results may shed new light on long-standing issues of BV chemistry and catalysis in biological systems.

Supporting Information

UV-Vis spectra of different BV/copper systems, BV/copper system in DMSO – UV-Vis and ^1H NMR spectra, speciation of Cu^{2+} in phosphate buffer, ESI-MS spcectum, scan rate analysis of BV and BV-Cu complex, list of Raman bands for BV.

Acknowledgements

This work was supported by the Ministry of Education, Science and Technological Development of the Republic of Serbia (III43010). We acknowledge networking support from the COST Action FeSBioNet (Contract CA15133). We thank Prof. Ana Popović-Bijelić and Prof. Miloš Mojović (EPR Laboratory, Faculty of Physical Chemistry, University of Belgrade) for acquiring low temperature EPR spectra. D.M.S was supported by Magbiovin project (FP7-ERA Chairs-Pilot Call-2013, Grant Agreement: 621375).

Conflict of Interest The authors declare that they have no competing interests.

References

(1) Bhuyan, J., Metalloisoporphyrins: from synthesis to applications Dalton Trans.2015, 44, 15742-15756.

(2) Balch, A. L.; Mazzanti, M.; Noll, B. C.; Olmstead, M. M., Geometric and electronic structure and dioxygen sensitivity of the copper complex of octaethylbilindione, a biliverdin analog. J. Am. Chem. Soc. 1993, 115, 12206-12207.

(3) Zhang, L., Heme biology: the secret life of heme in regulating diverse biological processes. World Scientific Publishing Company: Singapore, 2011.

(4) Chen, D.; Brown, J. D.; Kawasaki, Y.; Bommer, J.; Takemoto, J. Y., Scalable production of biliverdin IXα by Escherichia coli. BMC biotechnol. 2012, 12, 89.

(5) Cornelius, C., Biliverdin in biological systems. In One Medicine: Ryder O.A., Byrd M. L., Eds.; Springer: Berlin, Heidelberg, 1984;Chapter 27 pp 321-334.

(6) Sóvágó, I.; Harman, B.; Kolozsvári, I.; Matyuska, F., Complex-formation and redox reactions of bilirubin and biliverdin with zinc (II), cadmium (II) and copper (II) ions. Inorganica Chim Acta 1985, 106, 181-186.

(7) Goncharova, I.; Urbanová, M., Vibrational and electronic circular dichroism study of bile pigments: Complexes of bilirubin and biliverdin with metals. Anal. Biochem. 2009, 392, 28-36.

(8) (a) Asad, S. F.; Singh, S.; Ahmad, A.; Hadi, S., Bilirubin-Cu (II) complex degrades DNA. Biochim. Biophys. Acta 1999, 1428, 201-208; (b) Asad, S. F.; Singh, S.; Ahmad, A.; Khan, N. U.; Hadi, S., Prooxidant and antioxidant activities of bilirubin and its metabolic precursor biliverdin: a structure–activity study. Chem. Biol. Interact. 2001, 137, 59-74.

(9) (a) Fischer, B. E.; Haring, U. K.; Tribolet, R.; Sigel, H., Metal ion/buffer interactions. FEBS J. 1979, 94, 523-530; (b) Nagaj, J.; Stokowa-Sołtys, K.; Kurowska, E.; Frączyk, T.; Jeżowska-Bojczuk, M.; Bal, W., Revised coordination model and stability constants of Cu (II) complexes of tris buffer. Inorg. Chem. 2013, 52, 13927-13933.

(10) (a) McDonagh, A. F.; Palma, L. A., Preparation and properties of crystalline biliverdin IXα. Simple methods for preparing isomerically homogeneous biliverdin and [14C] biliverdin by

using 2, 3-dichloro-5, 6-dicyanobenzoquinone. Biochem. J. 1980, 189, 193-208; (b) Krois, D.; Lehner, H., Helically fixed chiral bilirubins and biliverdins: a new insight into the conformational, associative and dynamic features of linear tetrapyrrols. J. Chem. Soc., Perkin Trans. 2. 1993, 7, 1351-1360.

(11) Phillips, S.; Noll, B. C.; Olmstead, M. M.; Balch, A. L., Oxidation of copper (II) hydroxyporphyrin (oxophlorin); oxidative ring opening and formation of an ester-linked, dinuclear copper complex. Can. J. Chem. 2001, 79, 922-929.

(12) (a) Celis, F.; Campos-Vallette, M.; Gómez-Jeria, J.; Clavijo, R.; Jara, G.; Garrido, C., Surface-enhanced Raman scattering and theoretical study of the bilichromes biliverdin and bilirubin. *Spectrosc. Lett.* **2016,** *49*, 336-342; (b) He, J.; Lu, X. D.; Zhou, X.; Yu, N. t.; Chen, Z., Surface-enhanced Raman spectroscopy of bilirubin-metal ion complexes. *Biospectroscopy*. **1995,** *1*, 157-162; (c) Hu, J.; Wang, T.; Moigno, D.; Wumaier, M.; Kiefer, W.; Mao, J.; Wu, Q.; Niu, F.; Gu, Y.; Chen, Q., Fourier-transform Raman and infrared spectroscopic analysis of dipyrrinones and mesobilirubins. *Spectrochim. Acta A Mol. Biomol. Spectrosc.* **2001,** *57*, 2737-2743.; (d) Hu, J.-M.; Liang, E.-J.; Duschek, F.; Kiefer, W., Resonance Raman spectroscopic study of free brilirubin and brilirubin complexes with copper (II), silver (I) and gold (III). *Spectrochim. Acta A Mol. Biomol. Spectrosc.* **1997,** *53*, 1431-1438.

(13) Chen, J.; Hu, J.-m.; Sheng, R.-s., Surface-enhanced Raman spectroscopy of free bilirubin and bilirubin complexes with transition metals iron (II), nickel (II) and cobalt (II). *Spectrochim. Acta, Part A.* **1994,** *50* (5), 929-936.

(14) Tao, S.; Yu, L.-J.; Wu, D.-Y.; Tian, Z.-Q., Raman Spectra of Amino Wagging Vibrational Modes in p-π-Conjugated Molecules. Acta Phys.Chim. Sin. 2013, 29, 1609-1617.

(15) (a) He, J.; Lu, X. D.; Zhou, X.; Yu, N. t.; Chen, Z., Surface-enhanced Raman spectroscopy of bilirubin-metal ion complexes. Biospectroscopy 1995, 1, 157- 162; (b) Hu, J.-M.; Liang, E.-J.; Duschek, F.; Kiefer, W., Resonance Raman spectroscopic study of free brilirubin and brilirubin complexes with copper (II), silver (I) and gold (III). Spectrochim. Acta A Mol. Biomol. Spectrosc. 1997, 53 (9), 1431-1438.

(16) (a) Yunxia, Y.; Lihua, W.; Weichen, S.; Yinqun, H., Effects of Different Ligands on Fluorescent Properties of Nd3+ Organic Complexes. Rare Metal Mat. Eng. 2014, 43, 2359-

2364; (b) Zhang, Y.-M.; Zhang, X.-J.; Xu, X.; Fu, X.-N.; Hou, H.-B.; Liu, Y., Rigid Organization of Fluorescence-Active Ligands by Artificial Macrocyclic Receptor to Achieve the Thioflavin T-Amyloid Fibril Level Association. J. Phys. Chem. B. 2016, 120, 3932-3940.

(17) Sivaraman, G.; Iniya, M.; Anand, T.; Kotla, N. G.; Sunnapu, O.; Singaravadivel, S.; Gulyani, A.; Chellappa, D., Chemically diverse small molecule fluorescent chemosensors for copper ion. Coord. Chem. Rev. 2018, 357, 50-104.

(18) (a) Chen, Y.; Jiang, J., Porphyrin-based multi-signal chemosensors for Pb 2+ and Cu 2+. Org. Biomol. Chem. 2012, 10, 4782-4787; (b) Kano, K.; Sato, T.; Yamada, S.; Ogawa, T., Fluorescence quenching of water-soluble porphyrins. A novel fluorescence quenching of anionic porphyrin by anionic anthraquinone. J. Phys. Chem. 1983, 87, 566-569; (c) Prabphal, J.; Vilaivan, T.; Praneenararat, T., Fabrication of a Paper-Based Turn-Off Fluorescence Sensor for Cu2+ Ion from a Pyridinium Porphyrin. Chemistry Select. 2018, 3, 894-899.

(19) Mwakwari, S. C.; Wang, H.; Jensen, T. J.; Vicente, M. G. H.; Smith, K. M., Syntheses, properties and cellular studies of metallo-isoporphyrins. J. Porphyr. Phthalocyanines. 2011, 15, 918-929.

(20) Bertini, I.; Luchinat, C.; Parigi, G., Solution NMR of paramagnetic molecules: applications to metallobiomolecules and models. Elsevier: 2001; Vol. 2.

(21) Godziela, G. M.; Goff, H. M., Solution characterization of copper (II) and silver (II) porphyrins and the one-electron oxidation products by nuclear magnetic resonance spectroscopy. J. Am. Chem. Soc. 1986, 108, 2237-2243.

(22) Stoll, S.; Gunn, A.; Brynda, M.; Sughrue, W.; Kohler, A. C.; Ozarowski, A.; Fisher, A. J.; Lagarias, J. C.; Britt, R. D., Structure of the biliverdin radical intermediate in phycocyanobilin: ferredoxin oxidoreductase identified by high-field EPR and DFT. J. Am. Chem. Soc. 2009, 131, 1986-1995.

(23) Koerner, R.; Olmstead, M. M.; Ozarowski, A.; Phillips, S. L.; Van Calcar, P. M.; Winkler, K.; Balch, A. L., Possible intermediates in biological metalloporphyrin oxidative degradation. Nickel, copper, and cobalt complexes of octaethylformybiliverdin and their conversion to a verdoheme. J. Am. Chem. Soc. 1998, 120, 1274-1284.

(24) Szterenberg, L.; Latos-Grażyński, L.; Wojaczyński, J., Metallobiliverdin Radicals—DFT Studies. Chem. Phys. Chem. 2003, 4, 691-698.

(25) Pistner, A. J.; Pupillo, R. C.; Yap, G. P.; Lutterman, D. A.; Ma, Y.-Z.; Rosenthal, J., Electrochemical, Spectroscopic, and 1O2 Sensitization Characteristics of 10, 10-Dimethylbiladiene Complexes of Zinc and Copper. J. Phys. Chem. A. 2014, 118, 10639-10648.

(26) Galliani, G.; Monti, D.; Speranza, G.; Manitto, P., Biliverdin as an electron transfer catalyst for superoxide ion in aqueous medium. Experientia. 1985, 41, 1559-1560.

(27) Sochr, J.; Švorc, Ľ.; Rievaj, M.; Bustin, D., Electrochemical determination of adrenaline in human urine using a boron-doped diamond film electrode. Diam. Relat. Mater. 2014, 43, 5-11.

(28) Lightner, D. A.; Holmes, D. L.; McDonagh, A. F., On the Acid Dissociation Constants of Bilirubin and Biliverdin pKa values from 13C NMR spectroscopy. J. Biol. Chem. 1996, 271, 2397-2405.

Nguyen KT, Rath SP, Latos-Grazyński L, Olmstead MM, Balch AL. Formation of a highly oxidized iron biliverdin complex upon treatment of a five-coordinate verdoheme with dioxygen. J Am Chem Soc. 2004 May 26;126(20):6210-1.

Alan L. Balch, Lechoslaw Latos-Grazynski, Bruce C. Noll, Marilyn M. Olmstead, Nasser Safari Isolation and characterization of an iron biliverdin-type complex that is formed along with verdohemochrome during the coupled oxidation of iron(II) octaethylporphyrin J. Am. Chem. Soc., 1993, 115 (20), pp 9056–9061

Coordination Patterns for Biliverdin-Type Ligands. Helical and Linked Helical Units in Four-Alan L. Balch, Marinella Mazzanti, Bruce C. Noll, Marilyn M. Olmstead. Coordinate Cobalt and Five-Coordinate Manganese(III) Complexes of Octaethylbilindione. J. Am. Chem. Soc., 1994, 116 (20), pp 9114–9122

Alan L. Balch, Bruce C. Noll, Edward P. Zovinka Structural characterization of zinc(II) complexes of octaethyloxophlorin dianion and octaethyloxophlorin radical anion. J. Am. Chem. Soc., 1992, 114 (9), pp 3380–3385

Spasojević I, Batinić-Haberle I, Stevens RD, Hambright P, Thorpe AN, Grodkowski J, Neta P, Fridovich I. Manganese(III) biliverdin IX dimethyl ester: a powerful catalytic scavenger of

superoxide employing the Mn(III)/Mn(IV) redox couple. Inorg Chem. 2001 Feb 12;40(4):726-39.

Feliz M, Ribó JM, Salgado A, Trull FR, Vallò MA. On the 1H NMR Spectra of Biliverdins with Free Propionic Acid Substituents Monatshefte Chemie 120, 445451 (1989)

Peeks MD1, Tait CE2, Neuhaus P1, Fischer GM1, Hoffmann M1, Haver R1, Cnossen A1, Harmer JR2, Timmel CR2, Anderson HL1. Electronic Delocalization in the Radical Cations of Porphyrin Oligomer Molecular Wires.J Am Chem Soc. 2017 Aug 2;139(30):10461-10471.

Mahmudur Rahman and H. James Harmon Inhibition of aggregation of meso-tetra(4-sulfonatophenyl)-porphyrin (H4TPPS) by urea Journal of Porphyrins and PhthalocyaninesVol. 11, No. 02, pp. 125-129 (2007)

Božić B1, Korać J2, Stanković DM3, Stanić M2, Popović-Bijelić A4, Bogdanović Pristov J2, Spasojević I5, Bajčetić M6. Mechanisms of redox interactions of bilirubin with copper and the effects of penicillamine. Chem Biol Interact. 2017 Dec 25;278:129-134.

Pierloot K1, Zhao H, Vancoillie S. Copper corroles: the question of noninnocence. Inorg Chem. 2010 Nov 15;49(22):10316-29.

Wasbotten I1, Ghosh A. Biliverdine-based metalloradicals: sterically enhanced noninnocence. Inorg Chem. 2006 Jun 26;45(13):4914-21.

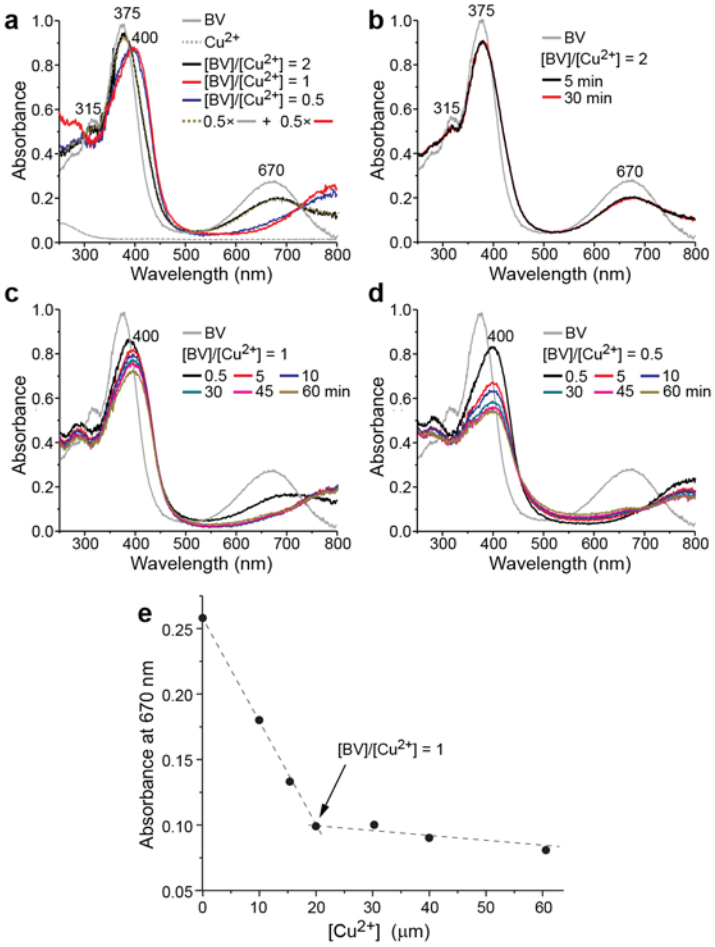

Figure 1. Changes in UV-Vis spectra of biliverdin (BV) in the presence of Cu^{2+} in phosphate buffer (50 mM; pH 7.4). (**a**) Different concentration ratios under anaerobic conditions (Ar atmosphere). Spectra were recorded after 5 min of incubation and remained stable for at least 60 min. (**b**) The system with [BV]/[Cu^{2+}] = 2 molar ratio under aerobic conditions. (**c**) [BV]/[Cu^{2+}] = 1 under aerobic conditions. (**d**) [BV]/[Cu^{2+}] = 0.5 under aerobic conditions. (**e**) Absorbance titration curve. Spectra were obtained after 5 min incubation period. In all experiments [BV] = 20 μM.

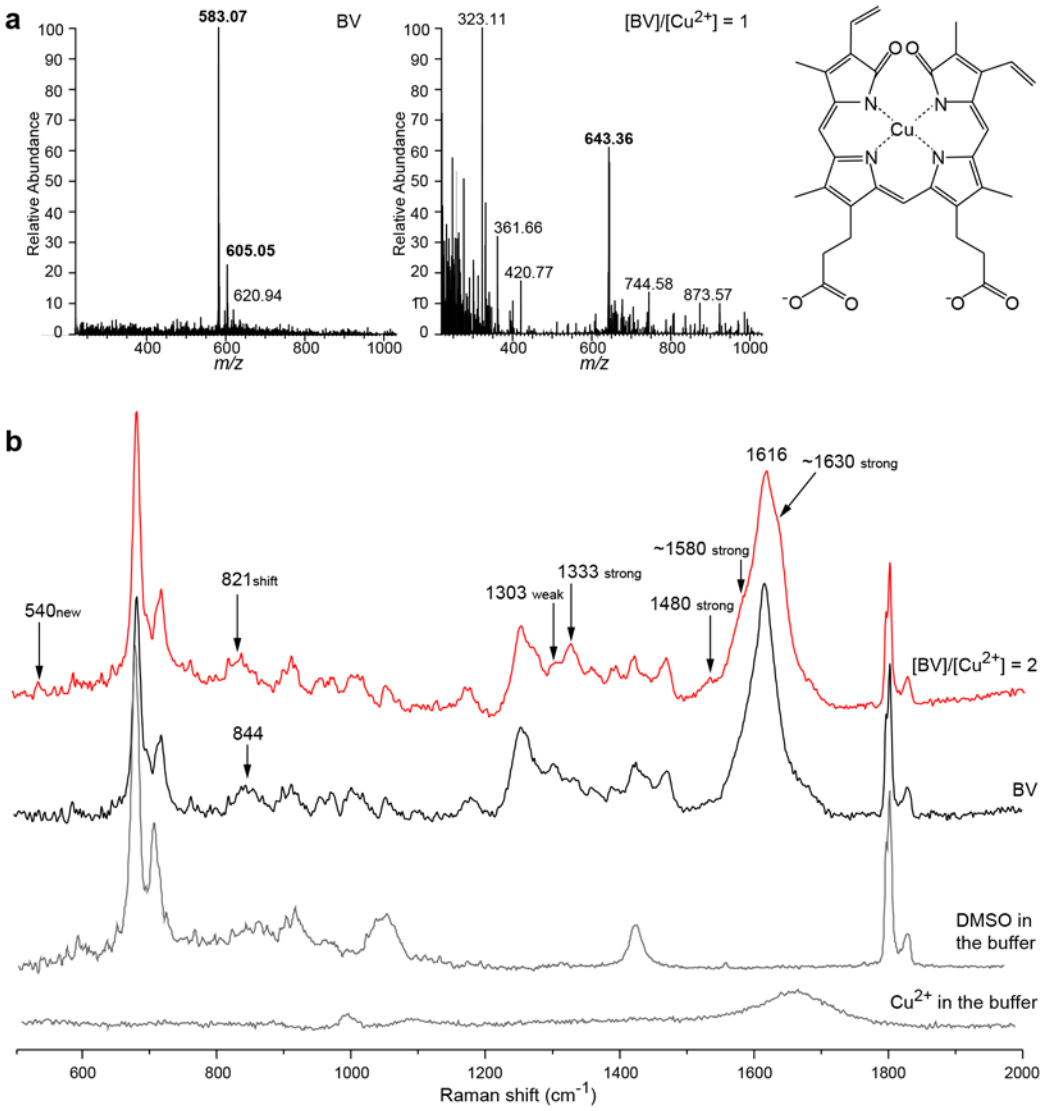

Figure 2. Structural analysis of biliverdin (BV) interactions with copper ions in phosphate buffer (50 mM; pH 7.4). (**a**) ESI-MS spectra, full scan positive mode. Proposed structure of the BV-Cu complex is illustrated on the right. The concentrations of BV and copper ions were 20 μM. (**b**) Raman spectra of BV (1 mM) and [BV]/[Cu^{2+}] = 2 system. Raman spectra of Cu^{2+} (0.5 mM) and phosphate buffer are presented for reference. Fluorescence-corrected spectra were obtained after 5 min incubation period using the λ = 532 nm laser excitation line.

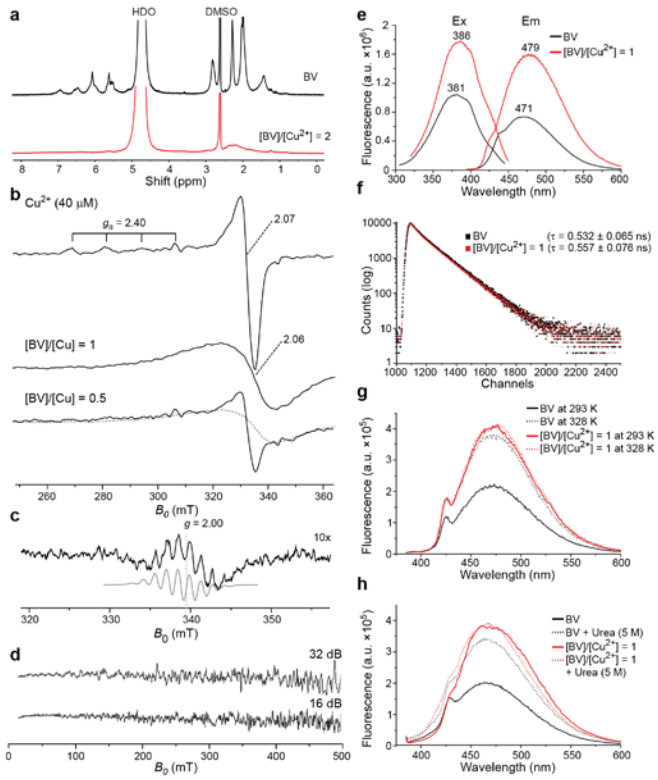

Figure 3. Paramagnetic properties of BV-Cu systems in phosphate buffer (50 mM; pH 7.4). (**a**) ^{1}H NMR spectra of BV (0.3 mM) with or without Cu^{2+} (0.15 mM) in the buffer prepared with D_2O. BV stock (20 mM) was prepared in DMSO. The acquisition of spectra was initiated after 5 min of incubation. (**b**) 30 K EPR spectra (perpendicular-mode) of 40 μM Cu^{2+} in the absence or the presence of BV (40 or 20 μM). Dashed line – the signal of the [BV]/[Cu] = 1 system divided by 2. (**c**) Room-T EPR spectrum of [BV]/[Cu] = 1 system. The spectrum was obtained via 10 accumulations (baseline corrected). Gray line - spectral simulation. (**d**) 25.5 K EPR spectra (parallel-mode) of 40 μM Cu^{2+} in the presence of 40 μM BV ([BV]/[Cu] = 1). Power was 32 and 16 dB. For low-T EPR, samples were frozen in liquid N_2 after 5 min incubation. (**e**) Excitation and emission fluorescence spectra of BV and [BV]/[Cu^{2+}] = 1 system. The concentrations of BV and Cu^{2+} in the sample were 10 μM. The acquisition of spectra was initiated after 5 min of incubation. (**f**) Fluorescence decay profile of BV and BV-Cu complex. Lifetime (τ) is presented as mean ± standard deviation. (**g**) Emission spectra of BV (λ_{ex} = 381 nm) and BV/Cu^{2+} (λ_{ex} = 386 nm) at two temperatures. (**h**) Emission spectra of BV (λ_{ex} = 381 nm) and BV/Cu^{2+} (λ_{ex} = 386 nm) in the absence and the presence of 5 M u

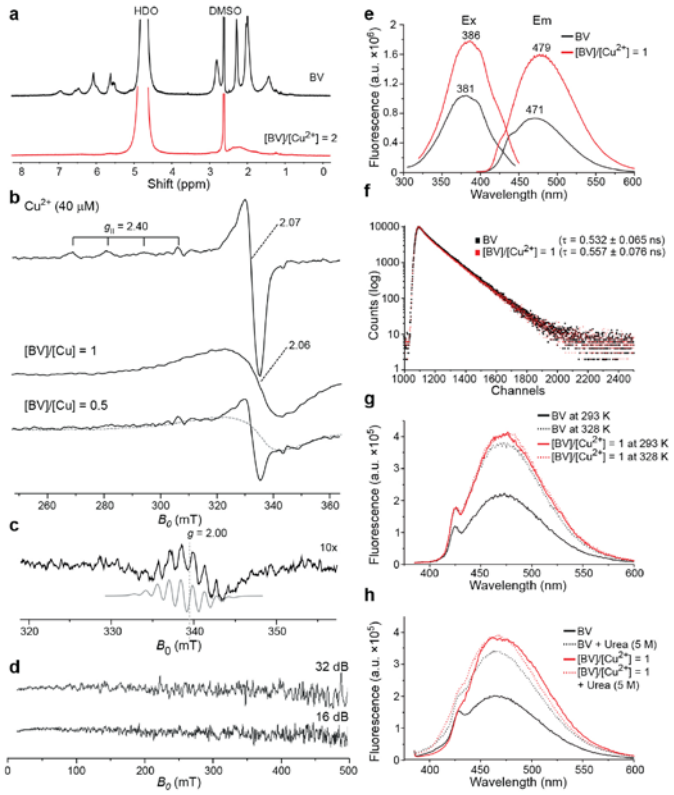

Figure 4. Redox properties of BV/Cu systems in phosphate buffer (50 mM; pH 7.4). (**a**) Cyclic voltammograms of BV and BV-Cu complex at a boron-doped diamond electrode (scan rate 0.1 V/s). Concentrations of BV and Cu^{2+} were 0.4 mM and 0.2 mM, respectively. Oxidation/anodic peak current potentials (E_{pa}) are labeled. (**b**) Differential pulse voltammograms (increment, 0.004 V; pulse width, 0.05 s; sample width, 0.01 s; quiet time, 2 s). (**c**) Consumption of molecular oxygen in BV solutions following addition of Cu^{2+}, or the addition of Cu^{1+} to phosphate buffer. The trace without Cu addition is presented for reference. In all experiments [BV] = 200 µM. (**d**) UV-Vis spectra of BV with Cu^{2+} and Cu^{1+} under anaerobic and aerobic conditions. The signals are compared to the spectra of analogous BV/Cu^{2+} systems. Cu^{1+} does not show detectable absorbance at the applied concentration. (**e**) The effects of reducing agent – ascorbate (Asc) on BV-Cu complex. (**f**) The effects of oxidizing agent – $KMnO_4$ on BV-Cu complex. Both, Asc and $KMnO_4$ did not affect the spectrum of free BV.

Synopsis

The coordinate/redox interactions of biliverdin with Cu^{2+} have been studies in phosphate buffer at pH 7.4. A set of experimental techniques - spectrophotometry, MS-ESI, Raman spectroscopy, ^{1}H NMR, EPR, fluorimetry and electrochemical methods point to formation of a stable 1:1 coordination complex with delocalized unpaired electron that most likely comes from the ligand. The complex is formally composed of biliverdin radical cation and Cu^{1+}.

For Table of Contents Only

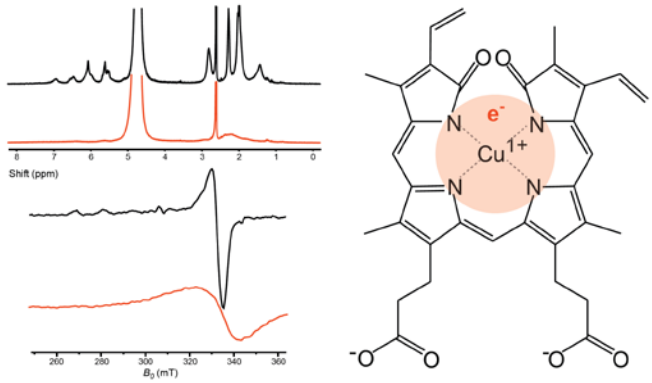

Supporting information

Biliverdin-copper complex at physiological pH

Milena Dimitrijević, Jelena Bogdanović Pristov, Milan Žižić, Dalibor Stanković, Danica Bajuk-Bogdanović, Marina Stanić, Snežana Spasić, Wilfred Hagen, Ivan Spasojević*

*E-mail: : redoxsci@gmail.com

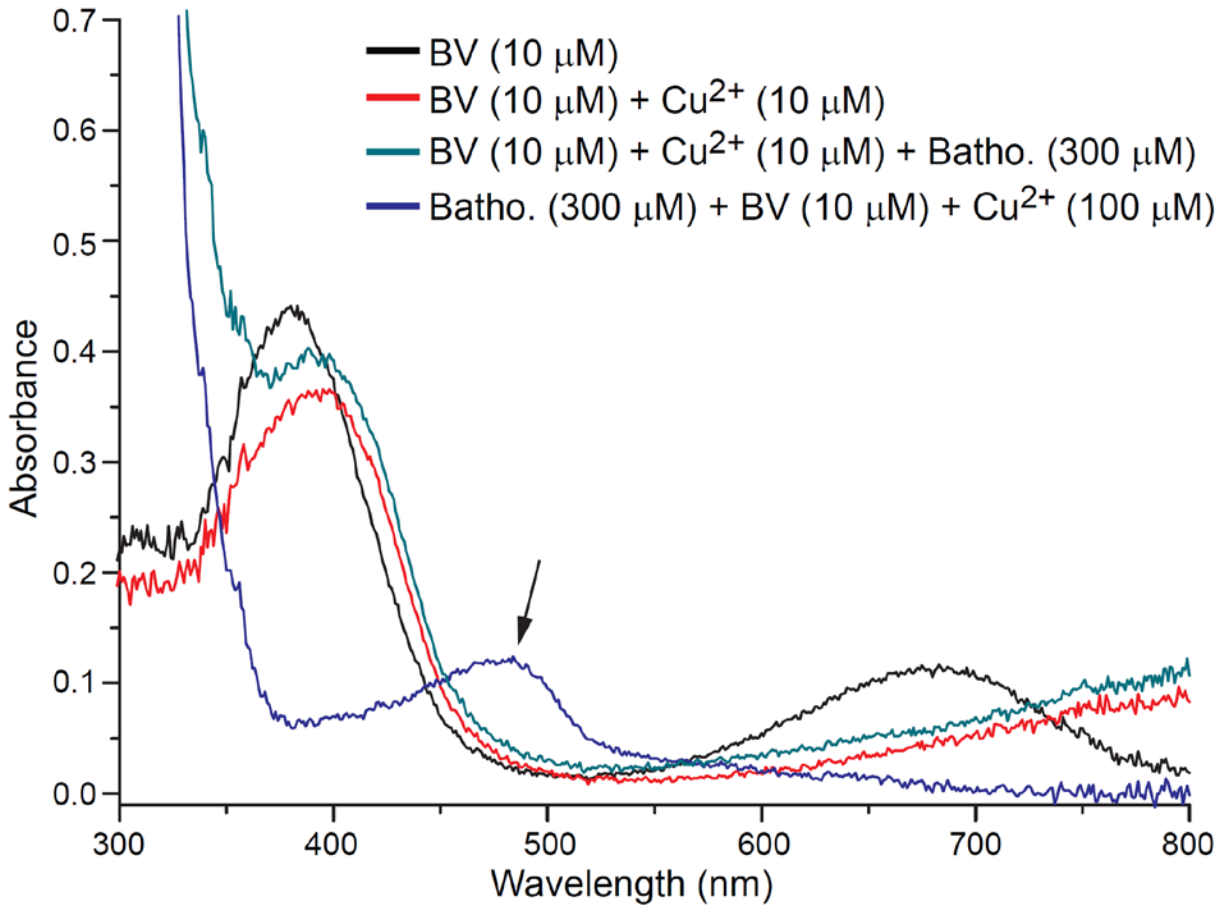

Figure S1. The stability of [BV]/[Cu^{2+}] = 1 system in the presence of copper chelating agent bathocuproine in phosphate buffer (50 mM; pH 7.4). Concentrations were: BV, 10 μM; Cu^{2+}, 10 μM; bathocuproine, 300 μM. Green line - BV and Cu^{2+} were incubated for 5 min before the addition of bathocuproine. Blue line - Cu^{2+} was added to the buffer with BV and bathocuproine (arrow – absorbance line of bathocuproine complex with copper).

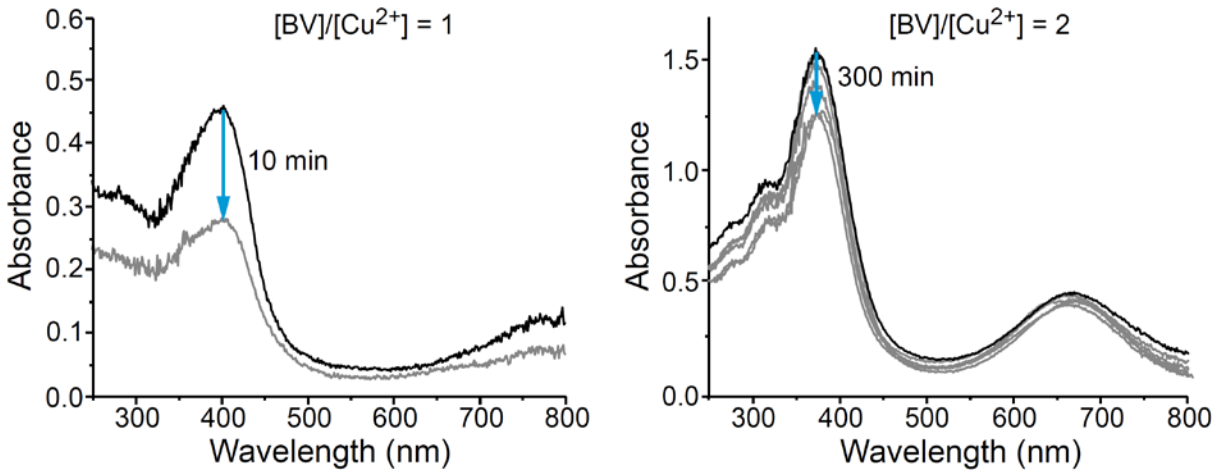

Figure S2. Changes in UV-Vis spectra of BV-Cu^{2+} systems prepared at high concentrations in 50 mM phosphate buffer, pH 7.4. Left: $[BV]/[Cu^{2+}] = 1$; $[BV] = [Cu^{2+}] = 0.3$ mM. Right: $[BV]/[Cu^{2+}] = 2$; $[BV] = 2$ mM; $[Cu^{2+}] = 1$ mM. Aliquots were taken from each system and diluted to lower final concentrations (10 or 40 μM, respectively), to allow spectra acquisition. It can be observed that the $[BV]/[Cu^{2+}] = 1$ system underwent degradation within 10 min, whereas the $[BV]/[Cu^{2+}] = 2$ system was relatively stable for 5 h.

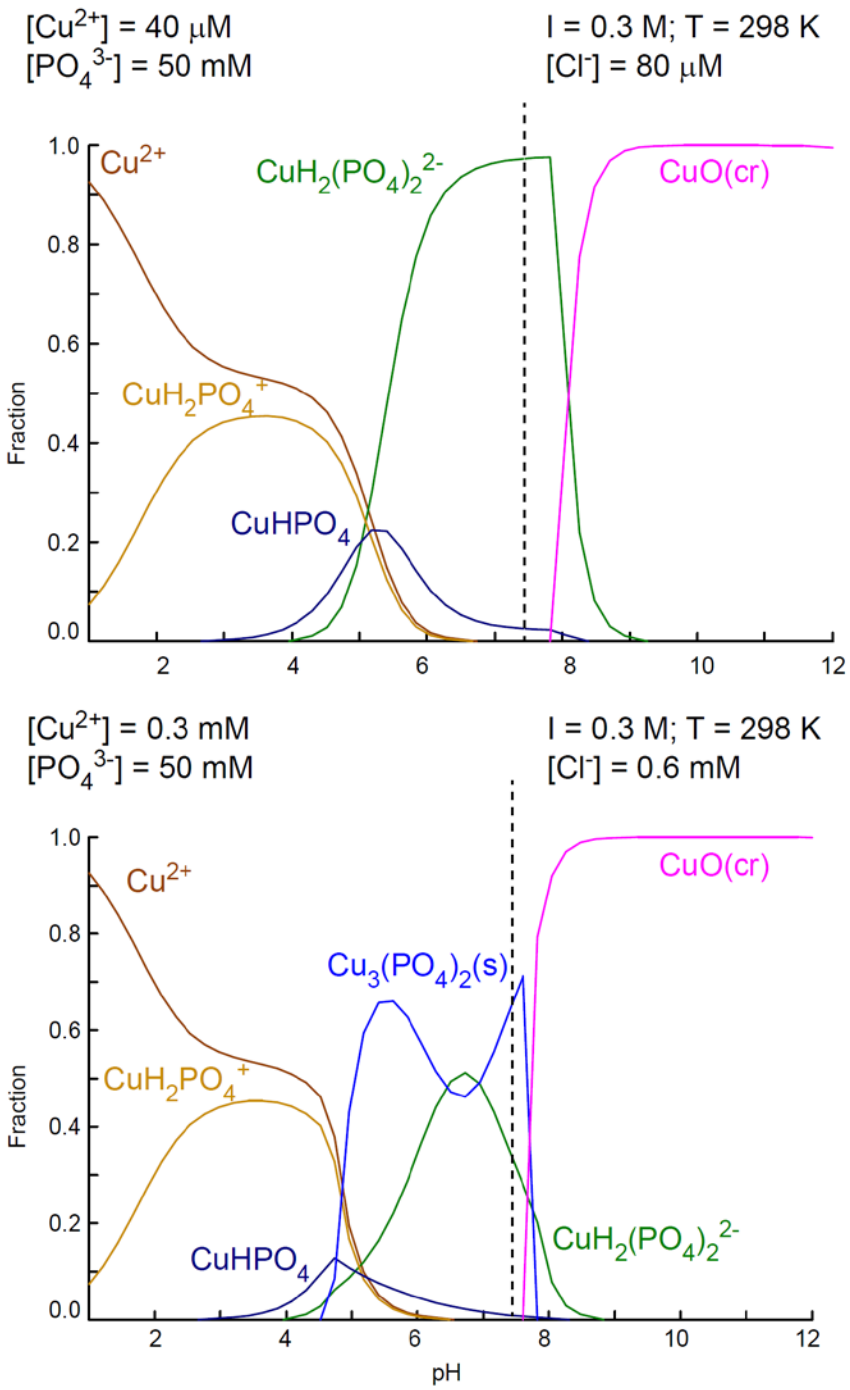

Figure S3. Speciation diagrams of Cu^{2+} in phosphate buffer (50 mM) at two concentrations – 40 μM (top) and 300 μM (bottom). Diagrams were prepared in Hydra-Medusa Software, using the presented parameters.

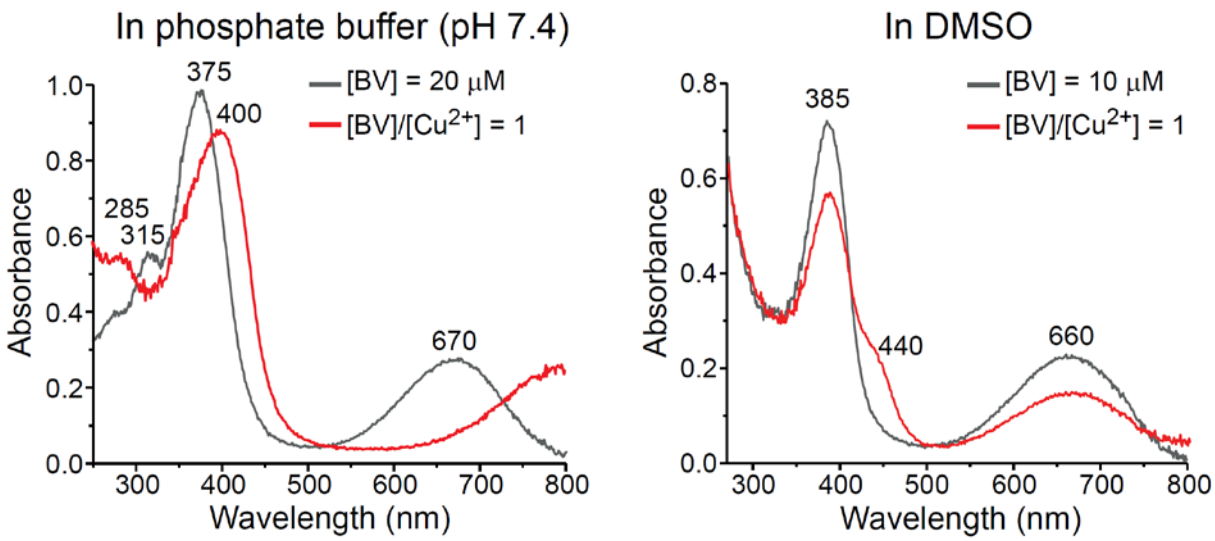

Figure S4. Comparison of UV-Vis spectra of biliverdin (BV) in the absence and the presence of Cu^{2+} in phosphate buffer (50 mM; pH 7.4) and in DMSO. Spectra were recorded after 5 min incubation period.

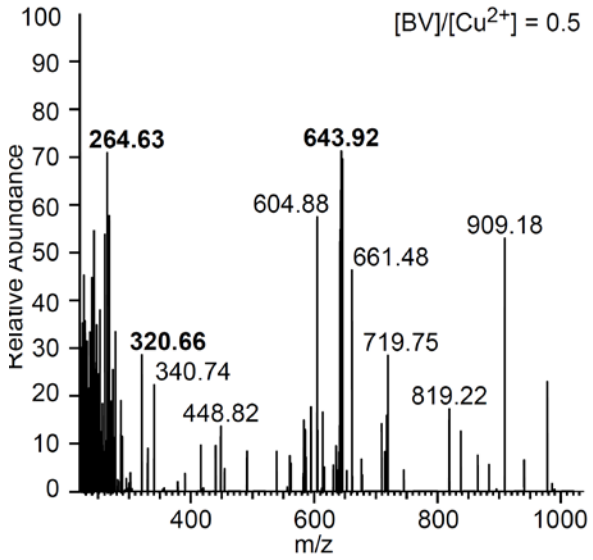

Figure S5. ESI-MS spectrum (full scan mode) of the system with [BV] = 20 μM and [Cu] = 40 μM. Assignation: *m/z* ~643, BV-Cu complex; *m/z* ~264, propentdyopent; *m/z* ~320, propentdyopent complex with copper.

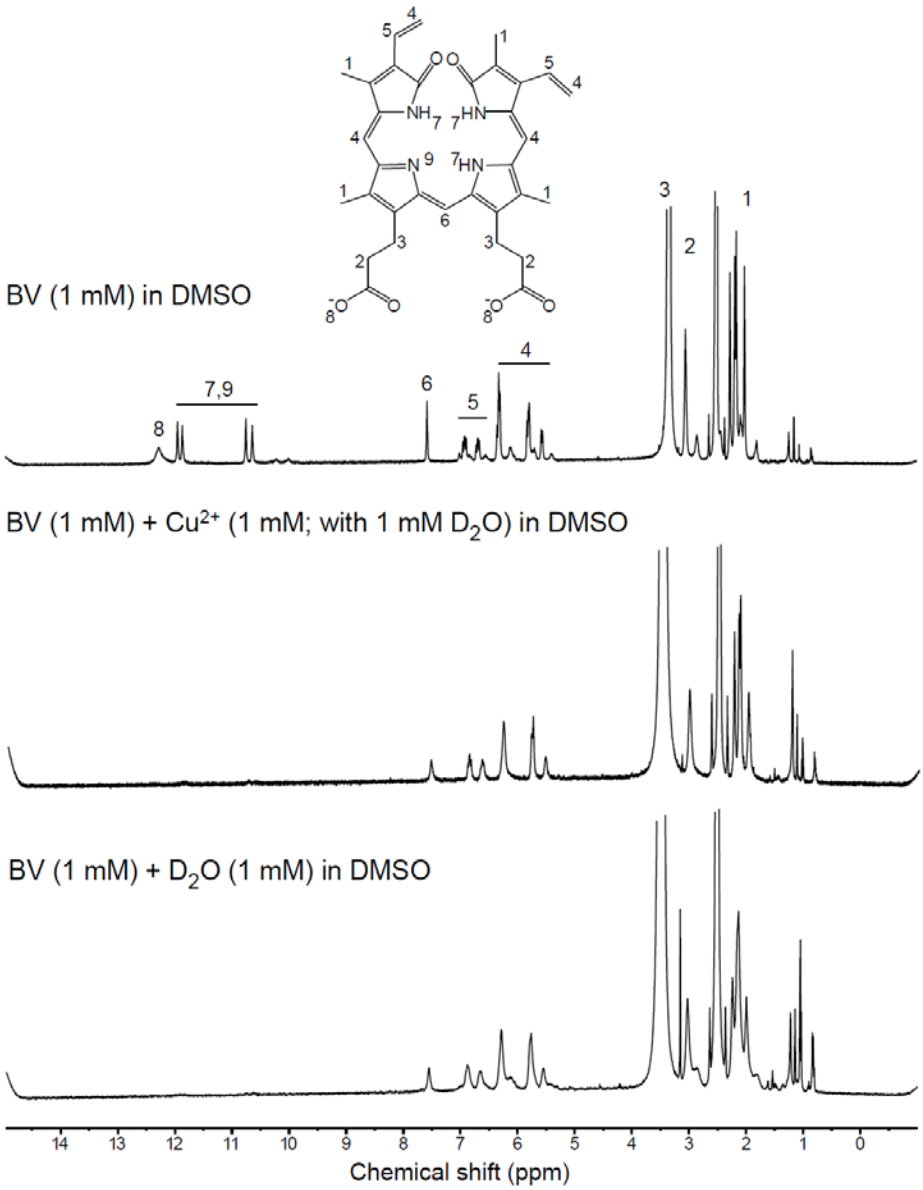

Figure S6. ^{1}H NMR spectra of biliverdin (0.3 mM) in DMSO-d6 in the absence or the presence of Cu^{2+} at equimolar concentration. The bottom spectrum was recorded in a copper-free system, with the equimolar amount of D_2O as in experiments with copper. It can be observed that Cu^{2+} and D_2O induced similar changes as D_2O alone. The peaks were assigned in accordance to previous reports[4, 22]. The signals labeled with 4 come from two types of protons (-CH= and $=CH_2$).

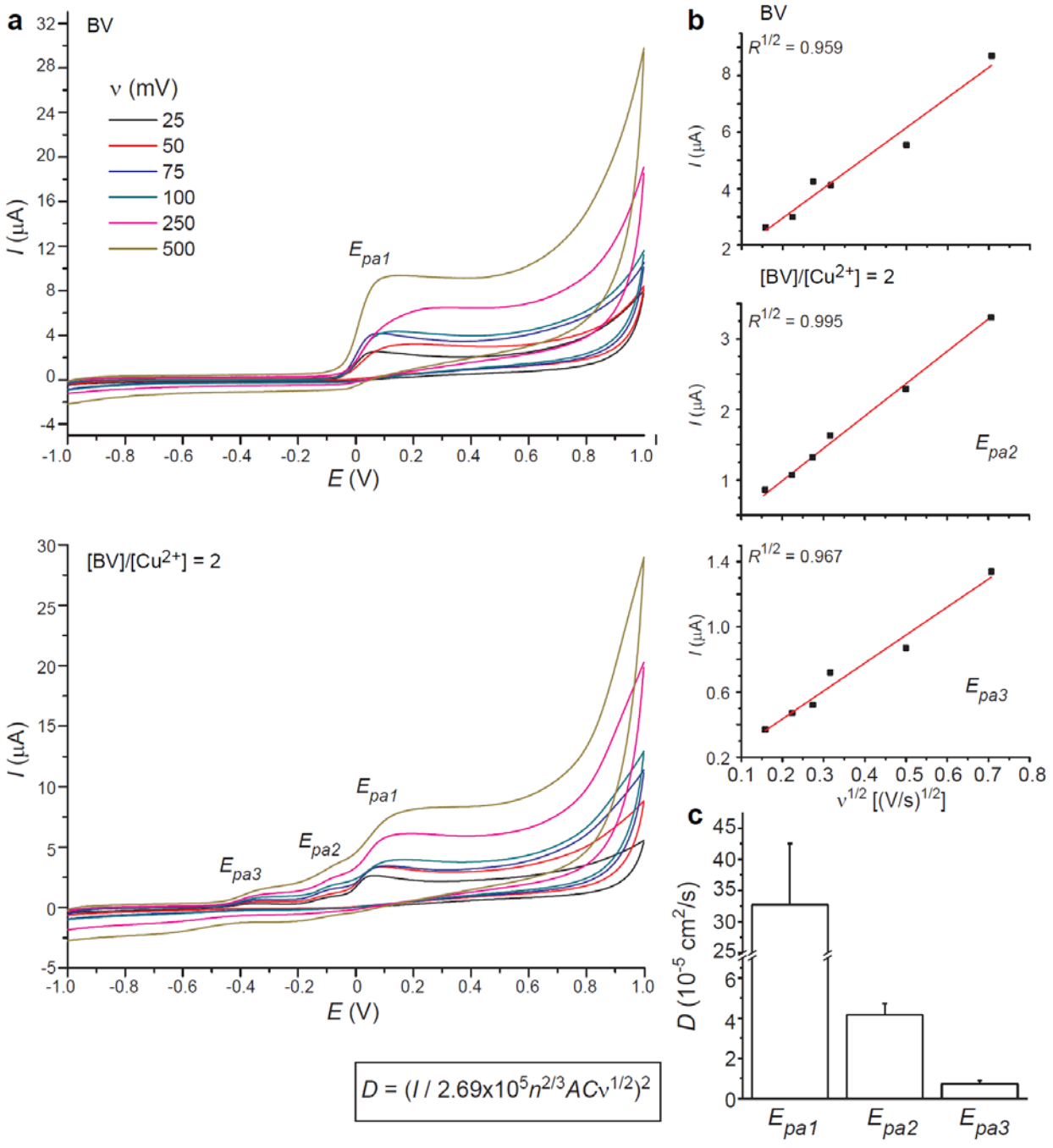

Figure S7. Scan rate analysis of BV and BV-Cu complex in phosphate buffer (50 mM; pH 7.4). (a) Cyclic voltammograms of BV (0.4 mM) in absence or presence of Cu^{2+} (0.2 mM) at the boron doped diamond electrode obtained at different scan rates (ν = 0.025–0.5 V/s). (**b**) The dependence between anodic peak currents I at potentials E_{pa1} (oxidation of BV), and E_{pa2} and E_{pa3} (oxidation of BV-Cu complex(es)) and $\nu^{1/2}$. Linear fit and R^2 values are presented. (**c**) D for BV and BV-Cu complex(es). Randles–Sevick equation (in the box): n, number of transferred e^-

(1e^- for all peak currents), *A*, area of the working electrode (0.0707 cm^2); *C*, concentration of redox species in solution ([BV] = 0.4 mM; [BV-Cu] = 0.2 mM). Results are presented as means (± standard deviation) of measurements made at various ν. All three *D* values were statistically different ($p < 0.001$; ANOVA with *post hoc* Duncan's test).

Table S1. Raman spectral lines that were observed for BV (1 mM), using the λ = 532 nm laser excitation line.

Line [cm^{-1}]	**Assignment**	**References**
1619	Lactam stretching	[12c]
1470	C–C deformation, likely between rings	[12c, 12d]
1443	Stretching CC, stretching CN	[12a]
1393	CH3 asymmetric deformation	[12a]
1362	CH3 deformation	[12a]
1331	In plane bending CH(CH_3)	[12a]
1303	CH wagging	[12a]
1254	Lactam ring	[12a]
1179	C–H twisting	[12c]
1101	Stretching C–C, stretching C–N	[12a]
1003	Asymmetric CH_3 deformation	[12a]
971	C–C stretching mixed with C–H rocking	[12c]
954	Stretching C–C–O	[13]
844	Stretching ring	[12a]
767	In plane ring deformation	[12a]
717	Out of plane ring deformation	[12a]
684	Out of plane bending C=O	[12a]